Inhibition of Fis1 by Novel Peptide Pep213 or Molecular Suppression Reverses Diabetic- and High Glucose-Induced Endothelial Dysfunction in Human Resistance Arteries

Mamatha Kakarla*,[1] John M. Egner*,[2] Jingli Wang,[1] Megan C. Harwig,[2] Kelsey Meacham,[2] Venkata K. Puppala[1] Benjamin C. Hofeld,[1] Leggy A. Arnold,[3] David Z. Trykall,[2] R. Blake Hill,[2] and Michael E. Widlansky[1,4]

1- Department of Medicine, Division of Cardiovascular Medicine, Medical College of Wisconsin, Milwaukee, WI
2- Department of Biochemistry, Medical College of Wisconsin, Milwaukee, WI
3- Department of Chemistry & Biochemistry and Milwaukee Institute for Drug Discovery, University of Wisconsin-Milwaukee, Milwaukee, WI
4- Department of Pharmacology, Division of Cardiovascular Medicine, Medical College of Wisconsin, Milwaukee, WI

Correspondence:

Michael E. Widlansky, MD, MPH, FACC, FAHA
Northwestern Mutual Professor of Cardiovascular Medicine
Academic Chief, Division of Cardiovascular Medicine
Professor of Medicine and Pharmacology
Medical College of Wisconsin
Hub for Collaborative Medicine, 5th Floor A5743
8701 W. Watertown Plank Road
Milwaukee, WI 53226
Phone: 414-955-6708
Email: mwidlans@mcw.edu

R. Blake Hill, PhD
Professor of Biochemistry
Medical College of Wisconsin
8701 W. Watertown Plank Road
Milwaukee, WI 53226
Phone: 414-955-5885
Email: rbhill@mcw.edu
* Authors contributed equally

Word Counts: 8808 (including cover page)

Abstract:

Background: Mitochondrial dysfunction drives the development of vascular endothelial dysfunction in type 2 diabetes (T2DM). Endothelial cells from either T2DM patients or healthy individuals exposed to high glucose exhibit increased fragmentation of mitochondrial networks, in part due to increased mitochondrial fission protein 1 (Fis1) expression, which drives mitochondrial reactive oxygen species production. Whether suppressing Fis1 expression or activity reverses endothelial dysfunction in resistance arteries from humans with T2DM and healthy vessels exposed to abnormal glucose concentrations remains unknown.

Methods: Resistance arterioles from the gluteal adipose pad were obtained from healthy humans and those with T2DM. Vessels underwent intra-luminal transfection with Fis1 siRNA (20 nM) and were exposed to normal glucose (NG, 5 mM), low glucose (LG, 2.5 mM) or high glucose conditions (HG, 33 mM). Endothelium-dependent vasodilation was measured by videomicroscopy. Vessel NO bioavailability was determined by DAF2-DA fluorescence. Immortalized human dermal microvascular endothelial cells (HMEC-1) cells were transfected with Fis1 siRNA to determine its impact on endothelial layer integrity and metabolism. We designed pep213 to inhibit Fis1 activity, and tested pep213's affinity for Fis1 using nuclear magnetic resonance and intrinsic tryptophan fluorescence titration experiments. Pep213's ability to reverse impaired endothelium-dependent vasodilation in T2DM and HG-exposed healthy vessels was determined by videomicroscopy.

Results: Fis1 knockdown improved endothelium dependent vasodilation in T2DM arterioles ($P=0.002$), and blocked HG ($P=0.0008$) and LG-induced ($P=0.0002$) impairment of endothelium-dependent vasodilation of healthy vessels. Fis1 knockdown preserved NO bioavailability and improved endothelial layer integrity of cells exposed to HG or LG ($P<0.001$). Fis1 knockdown had no significant effect on the expression of other mitochondrial dynamics or autophagy proteins, and had no effect on endothelial cell metabolism. Pep213 demonstrated low micromolar affinity

for Fis1 (3.3-7 μM). Tat sequence-linked pep213 improved endothelium-dependent vasodilation in T2DM ($P<0.001$) and non-T2DM vessels exposed to HG ($P<0.001$).

Conclusion: Reducing Fis1 expression reverses impaired vascular endothelial function and NO bioavailability in T2DM resistance arteries and in settings of abnormal glucose concentrations. Pep213, designed to inhibit Fis1, has similar favorable effects. These data support further development of therapeutics targeting Fis1 to reduce vascular complications in T2DM.

Introduction:

Impaired vascular endothelial function predates the development of macrovascular and microvascular disease in patients with type 2 diabetes (T2DM). Emerging data implicate abnormal mitochondrial form and function in the development of vascular endothelial dysfunction in humans with T2DM.[1, 2] Mitochondria in the endothelium of individuals with T2DM produce excessive superoxide. The excess superoxide is driven, in part, by greater polarization of the mitochondrial inner membrane.[2] Excessive mitochondrial reactive oxygen species (mtROS) production in the endothelium activates critical epigenetic changes and cell signaling pathways that lead to endothelial inflammation and vascular dysfunction.[3] We have previously shown that mitochondrial-targeted antioxidants or pharmacological agents dosed to partially depolarize the mitochondrial inner membrane reverse impaired endothelium-dependent vasodilation in resistance arterioles from humans with T2DM.[2, 4]

Unfortunately, the phase 3 clinical trials of anti-oxidant therapeutic approaches to prevent and treat vascular diseases have failed to verify positive effects seen in smaller physiological and/or non-randomized studies,[5, 6] and current pharmacological agents that target the mitochondrial inner membrane have toxicity profiles that preclude their clinical use.[7] Targeting proteins involved in mitochondrial fission represent a promising alternative approach based on prior work demonstrating (1) increased expression of mitochondrial fission 1 protein (Fis1) in endothelial cells obtained from humans with type 2 diabetes; (2) molecular knockdown of Fis1 or dynamin-related protein 1 (Drp1, which may bind Fis1 to induce mitochondrial fission) expression blocks high-glucose induced increases in mitochondrial superoxide production and impairment of phosphorylation of endothelium-derived nitric oxide synthase (eNOS) at its Ser1177 activation site; and (3) pharmacological and molecular knockdown of Drp1 reverse low-glucose induced endothelial dysfunction in human resistance arterioles.[1, 8] Fis1 as a pharmacological target is of particular interest given its role in mitochondrial dynamics appears

to be most highly active in the setting of pathological stimuli like hypoxemia and hyperglycemia.[9-12] In this set of investigations, we tested whether knockdown of Fis1 expression reversed impaired endothelium-dependent vasodilation and nitric oxide (NO) production in resistance vessels from patients with type 2 diabetes and in vessels from healthy individuals exposed acutely to high and low glucose concentrations. Additionally, we determined the effect of Fis1 knockdown on endothelial cell barrier function, oxygen consumption, and glycolysis under high or low glucose conditions. Finally, we designed and tested whether a novel peptide engineered to bind to Fis1 and block Fis-1 mediated fission favorably impacted endothelium-dependent vasodilation of small resistance arteries from humans with T2DM and from healthy human vessels exposed to high glucose concentrations. Our findings support our contention that pharmacological targeting of Fis1 might provide a useful therapeutic avenue for the challenge of vascular disease in T2DM.

Methods:

Subject Recruitment and Screening: We recruited 67 individuals with T2DM and healthy individuals (ages 21-75) without cardiovascular risk factors as previously described.[2, 13] Individuals with T2DM were either on medications to treat T2DM and/or met criteria for the diagnosis of T2DM American Diabetes Association.[14] Study methods were reviewed and approved by the Institutional Research Board of the Medical College of Wisconsin and all subjects signed a written informed consent form prior to proceeding with any study activities. All subjects were screened to assure they met study inclusion criteria. In all subjects, height and weight were measured and heart rates and blood pressures measured in triplicate. Subjects with or without T2DM were excluded if they had any of the following: known atherosclerotic disease (coronary artery disease, peripheral vascular disease, history of stroke or myocardial infarction), chronic liver disease, elevated plasma creatinine (> 1.5 mg/dl in men, > 1.4 mg/dl in women), a diagnosis of cancer in remission less than a year, regularly taking a blood thinner or

anti-platelet agent other than aspirin, or smoking cigarettes within a year of enrollment. Individuals without T2DM were also excluded if they had an LDL cholesterol ≥ 160 mg/dl or hypertension (blood pressure ≥ 140/90 mmHg) or if they were on medications to treat either of these entities. Vessels for the studies comparing the impact of pep213-tat and scrambled control peptides on endothelium dependent vasodilation (N=5 non-T2DM, N=4 T2DM) were obtained from discarded subcutaneous adipose tissue under a separate protocol reviewed and approved by the Medical College of Wisconsin's Institutional Research Board.

Human Resistance Artery Acquisition: Human resistance arteries from adipose samples were obtained from the upper outer quadrant of the gluteal adipose pad as previously described.[2, 8, 13, 15, 16] Briefly, following sterilization and anesthesia with 1% lidocaine, a 1-1.5 cm incision is made in the upper outer quadrant of the gluteal adipose pad. An approximately 8 cm^3 volume of adipose tissue was removed by sharp dissection. After achieving hemostasis, the wounds were closed with 1-2 absorbable deep dermal sutures and the epidermal layer closed using either Dermabond or steristrips.

Cell Culture: Immortalized human microvascular endothelial cells (HMEC-1) purchased from ATCC (Manassas, VA) were cultured in antibiotic-free MCDB131 (Life Technologies, Carlsbad, CA) supplemented with 10 mM Glutamine (Thermo Fisher Scientific, Waltham, MA), 10% FBS (Sigma-Aldrich, St. Louis, MO), 10 ng/mL Human EGF (Thermo Fisher Scientific), and 1µg/mL Hydrocortisone (Sigma-Aldrich). For assays involving high glucose (33 mM), normal glucose (5 mM), or low glucose (2.5 mM) conditions, antibiotic-free MCDB131 was supplemented with the above mentioned and glucose levels were adjusted by adding glucose and sterile PBS. Human dermal microvascular endothelial cells (HMEC) were purchased from Lonza (Basel, Switzerland) and supplemented with Microvascular Endothelial Cell Growth Medium-2 Bullet Kit (Lonza).

Transfection Protocols for Cultured Endothelial Cells and Human Vessels

Transfection of Fis1 and Drp1 siRNA and Scrambled Control into Cultured Cells Constructs for Fis1 and Drp1 siRNAs were acquired from Origene (Rockville, MD, sequences included in the supplemental material). Lipofectamine RNAi Max (Thermo Fisher Scientific) vehicle was added to 20 nM of RNAi constructs in Opti-MEM (Life Technologies). The mixture was diluted in culture media and incubated with HMEC-1 cells for four hours prior replacement with normal culture media. Cells were subsequently incubated for 24 hours before treatment and analyses. Following incubation, cells treated exposed to either high glucose for 6 hours or low glucose for 2 hours prior to measuring NO production, bioenergetics, protein expression, and endothelial layer integrity.

Transfection of Fis1 and Drp1 siRNA and Scrambled Controls in Human Resistance Arteries

Transfection of human resistance arteries with siRNA constructs was performed as previously described.[8, 13] Briefly, resistance arteries dissected from adipose tissue were suspended in a culture myograph chamber (204 CM, DMT, Ann Arbor). One end of the vessel was sutured onto a glass pipette within a micro-organ chamber. Prior to suturing the second end of the arteriole to a glass pipette, Fis1 siRNA, Drp1 siRNA (20 nM in optiMEM using Lipofectamine RNAiMax, Invitrogen) or control scrambled siRNA (20 nM) were gently injected, into the vessel lumen. The loose end of the vessel is then tied onto another glass pipette, and the vessel is suspended in the chamber and placed on a myograph stage bathed in physiological buffer at 37°C and pressurized to 60 mmHg. Following 4-6 hours of incubation, the siRNA is slowly washed out of the lumen over 24 hours at a low shear rate ($\tau < 5$ dyn/cm^2).

Measurement of Endothelium-Dependent Vasoactivity: Transfected resistance arteries from healthy individuals were exposed to either normal glucose conditions (NG, glucose level 5 mM), 2 hours of low glucose (LG, glucose level 2.5 mM) or 6 hours of high glucose (HG, glucose level

33mM). All studies in vessels from patients with T2DM were performed at 5 mM glucose. Vessels were pre-constricted approximately 50% of resting diameter with endothelin-1 (Sigma Aldrich, USA). The constricted arterioles are then exposed to acetylcholine (Ach) at serially increasing doses from 10^{-10} to 10^{-5} M, and changes in vessel diameter were measured using digital calipers and videomicroscopy. Following the 10^{-5} M dose, vessels were exposed to 200 µM papaverine to test the smooth muscle reactivity. Following a 30-minute washout period, the same arterioles were re-constricted and incubated with L-NG-nitroarginine methyl ester (L-NAME, 100µM), a direct inhibitor of nitric oxide synthase, for 30 minutes and vasodilation subsequently was remeasured following the exposure to Ach 10^{-10} to 10^{-5} M.

Measurements of Nitric Oxide (NO) Bioavailability:

Cells in Culture: To measure nitric oxide (NO) bioavailability in HMEC-1 cells and arterioles, a fluorescent NO marker, 4,5-diaminofluorescein diacetate (DAF2-DA from Cayman Chemical) was used. In a dark room, cells were incubated with or without 100 µM L-NAME for 2 hours followed by 15 minutes of incubation with DAF2-DA (5 µM) at 37°C. Fluorescence intensity was measured using a SPECTRAFluor Plus plate reader (Tecan, Morrisville, NC) using excitation and emission wavelengths of 485 nm and 535 nm, respectively.

Human Resistance Arteries: Two vessels were obtained from a subset of healthy subjects and each vessel was cut in half to allow for four experimental conditions which included transfection with Fis1 siRNA or Drp1 siRNA with and without concomitant exposure to L-NAME for 30 minutes and transfection with scrambled siRNA control with and without concomitant exposure to L-NAME at room temperature. Ach 10^{-5} M and DAF2-DA (5 µM final concentration) were subsequently added to each vessel and incubated at 37°C for 30 minutes. The arterioles were then washed with PBS buffer, mounted on a slide, and imaged by fluorescence microscopy. Untreated and unstained arterioles were used as controls for fluorescence background

interference. Both treated and control vessels were measured using the same gain settings and the results were analyzed using Meta Morph 7.8 software (Universal imaging, West Chester, PA).

Measurement of Endothelial Layer Integrity:

Human microvascular endothelial (HMEC-1) cells were seeded at 40,000 cells/ well and grown on gold electrode array plate (8W10E+, Applied Biophysics Inc.) until 50% confluent. The cells were pre-transfected with Fis-1 siRNA (20 nM) or scrambled siRNA (20 nM). On the days of experiments, the transfected cells were exposed to different glucose conditions: high glucose (33 mM) for 6 hours, normal glucose (5 mM) for 2 hours and low glucose (2.5 mM) for 2 hours. The integrity of the monolayers were checked at 64,000 Hz with less than 10 nF capacitance. The cells were then subjected to Electric Cell-substrate Impedance Sensing (ECIS) functional assay, and monolayer transepithelial electrical resistance (TEER) was measured in real time using an ECIS ZTheta Instrument (Applied Biophysics Inc., Troy, NY). Resistance was measured over the following frequencies, with 4,000 Hz as the standard: 125 Hz, 250 Hz, 500 Hz, 1,000 Hz, 2,000 Hz, 4,000 Hz, 8,000 Hz, 16,000 Hz, 32,000 Hz, and 64,000 Hz.

Mitochondrial Bioenergetic Measurements:

The XFe96 Analyzer (Seahorse Biosciences, North Billerica, MA, USA) was used to measure mitochondrial bioenergetics by measuring the oxygen consumption rate (OCR) and extracellular acidification rate (ECAR). HMEC-1 cells were seeded (20,000 cells/well) onto a 96-well Seahorse microplate 4-6 hours before treatment to let the cells adhere to the plate. Cells were pre-transfected with siRNA targeting Fis1 and siRNA scrambled control. The medium was aspirated and replaced with either high glucose for 6 hours or normal glucose or low glucose for 2 hours. The high, normal, or low glucose medium was removed and replaced with XF Base Medium Minimal Dulbecco's modified Eagle's medium (DMEM, pH 7.40) supplemented with 600

μL glucose 45%, 1.5 mL L-Glutamine (200 mM), and 1.5 mL sodium pyruvate (100 mM) with the final glucose concentration the same as the initial medium concentration. Cells were then incubated in a CO_2-free incubator at 37°C for 1 hour for temperature and pH calibration. During mitochondrial stress tests, the following drugs were sequentially injected in increments of 25 μL: Oligomycin A (2.5 μM final well concentration), FCCP (carbonyl cyanide 4-(trifluoromethoxy) phenylhydrazone, 1 μM final well concentration), and rotenone & antimycin A (1 μM final well concentration each). During glycolytic stress tests the following substances were sequentially injected in increments of 25 μL: glucose (10 mM final well concentration), oligomycin A (2.5 μM final well concentration), and 2-deoxyglucose (50 mM final well concentration).

Following these measurements, cells were fixed with 4% paraformaldehyde for 15 minutes and stained with DAPI (4',6-diamidino-2-phenylindole) at 1:500 of 1.5 μg/mL for 24 hours. Cell counts were obtained using automated cell counting on Cytation5 cell imaging multi-mode reader (BioTek, Vermont, USA) with OCR and ECAR measurements then normalized to cell number.

Measurement of Mitochondrial Proteins:

HMEC-1 cells were grown on a six well plates at 0.3 X 10^6 cells/well and transfected with siFis1 and siRNA. After transfecting for 4-6 hours, the medium was changed to normal cell culture medium and incubated overnight. Cells were treated either with HG (33 mM) for 6 hours, or NG (5 mM) or LG (2.5 mM) for 2 hours. The plates were then washed 2X with cell wash buffer and 50 μl RIPA lysis buffer (ProteinSimple, San Jose, CA) was added to each well. The cells were scraped gently on ice and transferred to a labelled tube. Lysates were centrifuged at 10,000 rpm for 10 minutes and snap frozen in liquid nitrogen and kept at -80°C overnight. The cell pellet and supernatant were thawed, vortexed briefly, and centrifuged at 10,000 rpm for 10 minutes. The supernatant was transferred to labelled tubes, protein concentration quantified by

Bradford assay, and protein expression evaluated by automated capillary electrophoresis-based immunodetection via WES (ProteinSimple). Proteins were analyzed and detected with the 12-230kDa WES separation module and 25 capillary cartridges. Lysates were diluted in 0.1X sample buffer in a 4:1 ratio of sample to fluorescent master mix, then denatured at 95°C for 5 minutes. For immunodetection, blocking buffer, primary antibody, secondary antibody, chemiluminescent substrate, samples, a biotinylated size marker and wash buffer were loaded in designated wells on the supplied microplate. The plate was centrifuged 5 min at 1000 X g then loaded into WES. Protein detection used default separation parameters. Compass for SW software (version 3.1.7, ProteinSimple) analyzed data and integrated specific antibody peaks. Across samples, protein expression was normalized to total protein. Total protein was analyzed in an addition WES assay with biotin-based protein labeling. Total protein was also analyzed using Compass for SW software as the integral of the antibody peaks. Control carryover samples between plates were used to correct for inter-plate signal intensity variability. The average quotient of antibody peak integrals with sample over total protein was taken.

NMR Titration Experiments:

To determine peptide binding affinities for Fis1, NMR titration experiments were performed similarly to chemical fragment titrations as described.[17] First, peptides were resuspended in Fis1 dialysate buffer (100 mM HEPES pH 7.4, 200 mM NaCl, 1 mM DTT, 0.02% v/v sodium azide) to a final concentration of 6 mM. Then, 220 µL of 50 µM ^{15}N–hFis1 and increasing amounts of peptide (0, 25, 50, 150, 400, 800, 1600, and 2000 µM) was prepared and loaded into 3 mm NMR tubes. For each sample, ^{1}H, ^{15}N HSQC spectra were collected at 25 ºC on a Bruker Avance II 600 MHz spectrometer equipped with a triple resonance z-axis gradient cryoprobe and SampleJet autosampler, which allowed automatic tuning, shimming, and data collection for each sample. ^{1}H, ^{15}N HSQC experiments consisted of 8 scans with 1024 and 300 complex points in the ^{1}H and ^{15}N dimensions, respectively. Spectra were processed with automated python scripts using NMRPipe

and chemical shifts were measured using TitrView and CARA software.[18, 19] Peptide binding affinity was determined by TREND analysis to each spectrum within the titration series.[20, 21] TREND reveals the changes in data by performing principal component analysis, where each concentration point is treated as a unique data point; here, the input is each ^{1}H, ^{15}N spectrum with increasing amounts of peptide. After performing principal component analysis, the principal component 1 (PC1) values are normalized to the highest PC1 value resulting in a range from 0 to 1. Then, the normalized PC1 values are plotted against peptide concentration and fit to a ligand depletion function with protein concentration held constant (Eq. 1)

Equation 1: $\Delta = \frac{\mathrm{d}_{max}*((K_d+p+l)-\left((K_d+p+l)^2-4*p*l\right)^{0.5})}{2*p}$, where Δ = adjusted chemical shift change, δ_{max} = maximum chemical shift perturbation, K_d = binding dissociation constant, p = [protein], and l = [ligand].

Spectral overlays were generated using XEASY software and Adobe Illustrator.

Synthesis of pep213:

Peptides pep213 (SHKHDPLPYPHFLL) and TAT-p213 (YGRKKRRQRRRGSGSGSSHKHDPLPYPHFLL) were all purchased from Genscript (Piscataway, NJ) with N-terminal acetylation and C-terminal amidation and >95% purity by HPLC. The TAT-p213 fusion peptide included a GSGSGS linker between the TAT cell penetrating sequence (YGRKKRRQRRR) and pep213.

Intrinsic Tryptophan Fluorescence:

Tryptophan fluorescence data was collected on a PTI Model #814 fluorimeter using a λ_{ex} of 295 nm and λ_{em} of 300 – 400 nm within Starna Cells 3-Q-10 quartz fluorometer rectangular cell with a 10 mm pathlength and excitation/emission slit widths of 4/6 nm, respectively. A concentrated stock of peptide (pep213) was resuspended in final hFis1 dialysate buffer and a concentration

series with the following points was prepared: 0, 1, 3, 7, 10, 30, 70, 100, 300, 700, and 1000 μM peptide. For each titration point, tryptophan emission spectra were collected on samples excluding Fis1 and then, 5 μL of 400 μM hFis1 was added to the sample for a final concentration of 10 μM hFis1 and tryptophan emission spectra were recollected. To account for buffer and tyrosine fluorescence background from the peptide, difference emission spectra were generated by subtracting the background fluorescence intensities from spectra lacking Fis1. The average emission wavelength at each peptide concentration was calculated according to Equation 3 and plotted as a function of the natural log of peptide concentration, which was fit to a Boltzmann sigmoidal model (Equation 4).[22]

Equation 3: $\langle \boldsymbol{\lambda} \rangle = \frac{\sum_{n=1}^{N} I_n * \lambda_n}{\sum_{n=1}^{N} I_n}$, where $\langle \boldsymbol{\lambda} \rangle$ = average emission wavelength, I_n = fluorescence intensity emitted at wavelength $\boldsymbol{\lambda}_n$, and the summation calculated from $\boldsymbol{\lambda}_n$ of 310 to 370 nm.

Equation 4: $\boldsymbol{\lambda} = A + \frac{(B-A)}{1+e^{\frac{K_D - p}{c}}}$, where $\boldsymbol{\lambda}$ = average emission wavelength, A = pre–transition phase, B = post–transition phase, K_D = equilibrium dissociation constant, p = natural log of the peptide concentration, and c = slope of the transition phase.

Impact of pep213 on Endothelial Cell NO Bioavailability and Endothelium-Dependent Vasodilation: Vessels from a subset of subjects with and without T2DM were selected at random for these studies. Vessels from healthy subjects were pre-treated with HG (33 mM) for six hours and subsequently exposed to 1 or 10 μM of pep213 attached to a TAT sequence to facilitate cellular uptake. Vessels from T2DM subjects were incubated under NG conditions (5 mM) and exposed to either 1 or 10 μM of pep213-TAT. Endothelium-dependent vasodilation with increasing doses of acetylcholine, smooth muscle reactivity to papaverine, and eNOS-

dependence of the vasodilatory response to acetylcholine using L-NAME were assessed as described previously.[2, 4, 8, 13, 15]

Statistical Analyses:

Statistical analyses were performed with either GraphPad Prism V7.03 (GraphPad Prism version 8.0.0 for Windows, GraphPad Software, San Diego, California, USA) or SigmaPlot Version 12.5 (Systat Software, San Jose, California, USA). $P < 0.05$ were considered statistically significant. Box and whisker plots present data as median, 25th-75th percentile box, and whiskers extending to 1.5 times the inter-quartile range. All other data are presented as mean ± SEM unless otherwise stated. All functional vessel data was analyzed by two-way ANOVA with post-hoc testing to determine the differences between groups (Dunnett's multiple comparison test) and dose-response (Tukey's multiple comparison tests). The TEER assay data and bioenergetics data were also analyzed by two-way ANOVA followed by post-hoc testing (Tukey's multiple comparison tests) to determine the differences between HG, LG, and NG treatments. DAF2-DA fluorescence intensity in human vessels, Fis1 knockdown-efficiency in HMEC-1 cells, and measurements of mitochondrial protein amounts by Western blot were analyzed by one-way ANOVA followed by Tukey's multiple comparisons to assess differences between groups. DAF2-DA fluorescence intensity in HMEC-1 cells transfected with siFis1 and scrambled siRNA were analyzed by two-way ANOVA followed by post-hoc testing (Tukey's multiple comparison tests). NO production and relative ratio of P-eNOS and β-actin in HMEC-1 cells stimulated with A23187 were analyzed using paired Students t-test.

Results:

Study Subject Characteristics: A total of 67 subjects (14 T2DM, 53 healthy controls) were recruited. A full description of the characteristics of subjects who participated in this project's studies is presented in **Table 1**. Our healthy subjects were significantly younger than the

subjects with T2DM (39±15 vs. 55±12 years, P=0.0002). Our healthy control subject group had a significantly lower body mass index, waist circumference, systolic blood pressure, fasting glucose, and glycosylated hemoglobin. Healthy subjects had higher HDL cholesterol levels as well. None of the healthy subjects were taking chronic cardiometabolic medications.

We additionally present the subject characteristics for each investigation involving humans vessels in **Supplemental Table 1** (subjects whose vessels were transfected with Fis1 siRNA or scrambled control and endothelium-dependent vasodilation tested), **Supplemental Table 2** (subjects whose vessels were transfected with Fis1 siRNA or scrambled control and NO bioavailability tested), **Supplemental Table 3** (subjects whose vessels were transfected with Drp1 siRNA or scrambled control and endothelium-dependent vasodilation tested), **Supplemental Table 4** (subjects whose vessels were transfected with Fis1 siRNA or scrambled control and NO bioavailability tested), and **Supplemental Table 5** (subjects whose vessels were exposed to pep213 and vasoactivity tested).

Impact of Suppression Fis1 or Drp1 on Endothelium-Dependent Vasodilation and NO Bioavailability in Human Vessels: Using our protocol, we measured vasodilation in healthy human resistance vessels incubated with glucose at concentrations experienced by T2DM patients (**Figure 1A-B**). Consistent with our earlier findings, both high (33mM) and low (2.5 mM) glucose blunted the endothelium-dependent vasodilatory response to acetylcholine that appeared primary related to eNOS activity based on inhibition with L-NAME. To address whether the mitochondrial fission protein Fis1 might be involved in this impairment, we transfected the healthy vessels with Fis1 siRNA that leads to approximately 30% reduction in Fis1 mRNA **(Supplemental Figure 1**). In these healthy human resistance vessels, transfection of Fis1 siRNA protected against HG and LG-induced impairments in endothelium-dependent vasodilation **(Figure 1A-B)**. Administration of L-NAME completely blocked this protective effect in both cases suggesting that Fis1 siRNA associated improvements are eNOS-dependent.

Consistent with this interpretation, Fis1 siRNA transfection also significantly increased the fluorescence of NO-sensitive dye DAF2-DA in vessels from healthy individuals exposed to HG [**Figure 2A**; n=9, P=0.04 for Fis1 siRNA versus all other exposures (scrambled control, scrambled control + LNAME, and Fis1 siRNA + L-NAME)] and LG (**Figure 2B**, n=8, P=0.01 for Fis1 siRNA vs. all other exposures). L-NAME completely abolished the increased in DAF2-DA fluorescence in both cases. These data support the concept that Fis1 silencing can improve vasodilation in an NO-dependent manner under stress conditions experienced by T2DM patients. We next asked whether Fis1 siRNA treatment could improve vasodilatory activity in resistance vessels from T2DM patients. Treatment with Fis1 siRNA reversed impaired endothelium-dependent vasodilation (**Figure 3;** n=6, P=0.002 overall). As with vessels from healthy subjects, the favorable effect of Fis1 siRNA transfection on vessels from diabetic subjects was completely attenuated by L-NAME. Fis1 siRNA transfection did not impact the papaverine effect on vasodilation in any of these studies (data not shown). We had similar findings with genetic silencing of Drp1 in vessels from healthy and diabetic individuals (Supplemental Results and Supplemental **Figures 2-4**) consistent with excessive mitochondrial fission playing an important role in impairing NO-dependent vasodilation in the diabetic endothelium.

Impact of Fis1 Transfection on Fis1 expression, NO production, eNOS activation, and Expression of Mitochondrial Protein Associated with Fission, Fusion, and Autophagy: HMEC-1 cells transfected with Fis1 siRNA showed a significant 70% reduction in Fis1 expression (**Supplemental Figure 5**). Confirming the responsiveness of HMEC-1 to stimulus that increases eNOS activation and NO bioavailability, calcium ionophore A23187 drove a significant increase in both eNOS phosphorylation at the Ser1177 activation site and DAF2-DA fluorescence intensity in non-transfected HMEC-1 cells (**Supplemental Figure 6A,** N=6, P=0.03; **6B,** N=4, P=0.02). Fis1 siRNA transfection also significantly increased DAF2-DA signal

from HMEC-1 cells stimulated with A23187 compared to transfection of scrambled control siRNA transfection (**Supplemental Figure 7,** N=7, P<0.0001). Knocking down Fis1 expression did not significantly change expression of mitochondrial proteins involved in mitochondrial fission, fusion, and autophagy including cytochrome c, MFN1, MFN2, Drp1, GABARAP, MFF, POLG, NDUF88, P62, OPA1, or AMP Kinase (**Supplemental Figure 8**). The lack of impact on expression of these proteins was apparent under HG, LG, and NG incubation conditions. High and low glucose did influence the expression of some of these proteins but Fis1 knockdown had no effect within a given glucose exposure.

Impact of Fis1 Knockdown and Endothelial Cell Layer Integrity: The impact of Fis1 suppression on endothelial cell layer integrity under HG and NG conditions is reported in **Figure 4A.** Under NG conditions, knockdown of Fis1 expression modestly but statistically significantly reduced endothelial cell layer resistance (P<0.05). Under HG conditions, endothelial cell layer resistance was significantly lower than resistance under NG conditions with or without Fis1 knockdown (P<0.001). Fis1 knockdown significantly increased resistance under HG conditions (P<0.0001) but remained lower than the resistance measured under NG conditions. Similar findings were found for LG (**Figure 4B**).

Impact of Fis1 Knockdown on Oxygen Consumption and Glycolysis: Knockdown of Fis1 had no effect on either the extracellular acidification rate or oxygen consumption regardless of glucose exposure (NG, HG, and LG; n=5 for all measurements, **Figure 5**) suggesting that inhibition of Fis1 does not significantly impact mitochondrial bioenergetics.

Determination of the Affinity of pep213 for Fis1: Previous work identified several potential Fis1 binding peptides by phage display screening against a truncated version of the protein.[23] We tested a subset of these peptides for binding to Fis1 and found weak affinity (high μM). From these data, we designed a novel peptide, pep213, that we reasoned might have higher affinity to

Fis1 and block its activity. To evaluate this, we titrated increasing amount of the peptide into an NMR sample of Fis1 uniformly labeled with the stable isotope ^{15}N. A superposition of the resulting ^{1}H-^{15}N HSQC spectra shows many signals change upon addition of pep213 indicating binding (**Figure 6A**). The resulting data can be globally fit to a single site binding model and gave an apparent K_D = 7 ± 2 μM (**Figure 6B)**. This affinity was confirmed by tryptophan fluorescence experiments in which changes in the tryptophan emission spectra upon addition of pep213 were fit to a binding isotherm to give a similar apparent K_D = 3.3 ± 0.1 μM (**Figure C**). Another peptide (pep213-scrambled) consisting of the same amino acid composition as pep213, but in random order, showed no chemical shift perturbations upon addition to ^{15}N-Fis1 at 2 mM indicating the Fis1-pep213 interaction is specific (**Figure 6D)**.

Impact of pep213 on Endothelium-Dependent Vasodilation in Human Resistance Vessels: Exposure to *pep213* attached to TAT peptide to facilitate cellular uptake resulted in a significant improvement in endothelium-dependent vasodilation in both vessels from healthy subjects exposed to high glucose (**Figure 7A**, N=6, P<0.0001 overall) and vessels from T2DM subjects (**Figure 7B,** N=4, P<0.05 overall). In both cases, treatment with L-NAME abolished the improvements seen with pep213-TAT. While pep213-TAT reversed high-glucose induced impairment of endothelium-dependent vasodilation and impaired endothelium-dependent vasodilation in vessels from subjects with T2DM, a scrambled peptide using the same amino acids in a random sequence had no effect on either set of vessels (**Figure 8** N=5, P<0.001 overall). No differences were seen in the papaverine responses (data not shown) in any of these studies suggesting pep213-TAT did not impact smooth muscle reactivity. Additionally, human microvascular endothelial cells exposed to pep213-TAT for one hour showed a significant increase in DAF2-DA fluorescence (**Supplemental Figure 9**, N=3, P=0.04).

Discussion:

These investigations reveal several novel findings. First, molecular inhibition of Fis1 blocks the unfavorable impacts of high- and low-glucose exposures on the ability human microvascular endothelial cells to produce NO, vasodilate in an endothelium-dependent manner, and maintain the endothelial cell layer barrier function. Additionally, molecular inhibition of Fis1 expression reverses impairment of endothelium-dependent vasodilation in human vessels from T2DM patients. These favorable effects occur without changes in endothelial cell metabolism or the expression of other proteins involved in mitochondrial fusion, fission, or autophagy. Additionally, using our knowledge of the structure of a critical binding site on Fis1, we designed a peptide with low micromolar binding affinity to Fis1 at this site, pep213, and verified its binding using two independent methods. Finally, we showed that pep213 is biologically active, increases NO bioavailability in human microvascular endothelial cells, and reverses high glucose-induced and type 2 diabetes-associated impairment of endothelium-dependent vasodilation in human resistance arteries in a nitric oxide synthase-dependent manner. These findings suggest a critical mechanistic role for excessive Fis1 expression and activity in the impairment of endothelial function in the settings of both acute and chronically abnormal glucose levels. Additionally, these data support the concept that a pharmacological therapy targeting to Fis1 holds promise for improving vascular health in patients with type 2 diabetes.

A strong rationale exists for exploring whether targeting mitochondrial proteins involved regulating the mitochondrial dynamics would lead to a favorable impact on human vascular endothelial function in patients with type 2 diabetes or patients exposed to high glucose concentrations. Properly balanced mitochondrial network dynamics are critical for maintaining normal mitochondrial function. Normal mitochondrial dynamics allow mitochondria to move to areas of increased metabolic demand, repair damaged mitochondria, maintain normal mitochondrial energetics, limit reactive oxygen species production, and isolate irreversibly

damaged mitochondrial components for autophagy.[24-28] The acute and chronic exposure to excessive nutrients, such as elevated glucose or free fatty acids, stimulates the mitochondrial network to undergo fission in multiple cells types, including human endothelial cells, leading to excessive mitochondrial ROS production.[1, 28-30] Seminal work in cultured endothelial cells demonstrates that high glucose driven excessive mitochondrial ROS production that leads both acute and chronic impairment endothelial cell function through cell signaling and epigenomic pathways.[3, 31] We have also previously demonstrated that reducing mitochondrial superoxide levels in resistance arteries from patients with type 2 diabetes reverses impaired endothelium-dependent vasodilation in human small resistance vessels.[2]

These data suggest that targeting mitochondrial dynamics proteins to reduce excessive mitochondrial fission could benefit vascular health in vessels acutely or chronically exposed to abnormal glucose levels. While there are multiple proteins involved in mitochondrial fusion and fission processes, Fis1, located on the outer mitochondrial membrane and docking protein for Drp1, has been repeatedly shown to be over-expressed in the setting of diabetes, acute high glucose exposure, or acute exposure to excessive free fatty acids in multiple cell types.[1, 32-35] While Fis1 is not necessary for all fission,[36] Fis1-Drp1 mediated fission appears to be preferred under conditions of cellular stress such as hypoxia and excessive glucose exposure.[9-12] Prior work in the human vasculature demonstrate Fis1 is overexpressed in endothelial cells from individuals with type 2 diabetes.[1] In addition, high glucose exposure leads to over-expression of Fis1 in cultured human aortic endothelial cells, and molecular silencing of Fis1 or Drp1 expression in human aortic endothelial cells exposed to high glucose results in an increase in phosphorylation of eNOS at its Ser1177 activation site.[1] Additionally, we previously showed that clinically relevant levels of low glucose exposure leads to mitochondrial fission in human endothelial cells and excessive mtROS production that can be reversed by suppressing mitochondrial fission protein activity.[8] Our new data significantly extends the translational

impact of prior work by showing that molecular inhibition of Fis1 reverses impaired endothelium-dependent vasodilation in intact human resistance arteries, increases NO bioavailability in these vessels, and protects endothelial cell layer integrity in the setting of abnormal glucose levels. In addition, we determined that targeting Fis1 does not impact endothelial cell mitochondrial metabolism or the expression of other mitochondrial proteins involved with dynamics or autophagy, reassuring observations when considering potential off-target effects of therapeutically targeting Fis1.

We found pep213, designed to bind Fis1 at a key interaction surface, both increased NO bioavailability in cultured endothelial cells and reversed both type 2 diabetes and high glucose-induced impairment of endothelium-dependent vasodilation. In concert with our molecular results, our data using the novel pep213 peptide support that direct pharmacological inhibition of Fis1 has favorable effects on the diabetic vasculature. Interestingly, several medications given as treatment of type 2 diabetes, two of which improve reduce cardiovascular risk in T2DM, also inhibit mitochondrial fission as an “off-target” effect by reducing Fis1 and/or Drp1 expression. Empagliflozin, and SGLT2 inhibitor with favorable effects on cardiovascular risk, mortality, and microvascular renal disease in T2DM patients,[37, 38] used in rat model of T2DM (OLEFT), reduced Fis1 over-expression in the model, reduced mitochondrial fission, and up-regulated mitochondrial superoxide dismutase, SOD2, in cardiac myocytes.[39] Metformin, a long-time first-line agent for T2DM glucose control with favorable cardiovascular effects, reduces atherosclerotic formation in ApoE knockout mice by suppressing Drp1-mediated fission.[40] The dipeptidyl peptidase 4 inhibitor vildagliptin, from a class of medications known to increase NO production, reduces expression of Fis1 and Drp1, reduces Drp1 translocation from the cytosol, and reduces mitochondrial fission and ROS production, while increasing NO production in the aortic endothelium of diabetic mice.[41] Interpreted within the framework of our presented data, these common anti-diabetes medications may have ameliorative vascular effects in T2DM in

part based on off target effects on the expression and/or interaction of Fis1 and Drp1. Whether these improvements are due to improved glycemic control or direct inhibition of Fis1 or Drp1 interaction merits future study.

Our study has some limitations. First, we focused primarily on the Fis1-Drp1 axis in regulating the vascular effects of T2DM and abnormal glucose exposures due to prior data supporting this axis as being most relevant in the setting of hyperglycemia and other pathological stimuli and our prior work supporting Fis1's pathophysiological role in the diabetic endothelium.[1, 9-12] Whether or not blocking Fis1 impairs interactions with Drp1 or with other mitochondrial docking proteins (Mff, MiD49/51) is unknown and merits future investigation. We did also not focus on mitochondrial fusion proteins (e.g. OPA1, Mfn1, Mfn2). Emerging data suggest Mfn2 expression downregulated in the tissues of patients with T2DM and Fis1 may also drive fission by inhibiting the GTPase activity of fusion proteins which may further reduce NO bioavailability.[1, 42-44] The fusion pathway's role in the regulation of human vascular endothelial function and its potential interaction with Fis1 merits also merits additional investigation. We did not perform osmotic controls with our experiments. However, we have done these controls with similar intact vessel and endothelial cell experiments on mitochondrial regulation of vascular function in our prior work and have never observed osmotic differences to influence our results.[4, 8] Balanced against these limitations is the novelty of our findings in highly disease relevant tissues from humans, and the development of novel intervention to blunt and reverse the adverse effects of diabetes on the human vasculature targeting the mitochondrial fission machinery.

Conclusion:

The work presented here demonstrates the critical role of Fis1 in regulating vascular endothelial function in intact resistance vessels from individuals with T2DM and in settings of

acute abnormal glucose levels. We used both molecular techniques as well as a novel peptide pep213, specifically designed in to block a key binding surface of Fis1, to demonstrate the importance of this interaction to vascular function in vessels from T2DM patients. We additionally showed that reducing Fis1 levels does not impact the levels of other important mitochondrial proteins or mitochondrial oxygen consumption while improving endothelial function. Taken together with earlier works, these data support further work into the pharmacological targeting of Fis1 to reduce vascular complications in T2DM.

Acknowledgement: We gratefully acknowledge Ms. Cathy Paddock and Dr. Peter Newman for training and access to the ECIS instrument for TEER measurements.

Sources of Funding: Dr. Puppala received support from GM089586. Dr. Hofeld is supported by R38HL143561. Dr. Hill receives support from HL128240 and GM067180. Dr. Widlansky receives support from HL128240, HL125409, HL144098, R38HL143561, and R61AT010680. Mr. Trykall was supported by T35HL0724485 and a participant the Medical College of Wisconsin's Molecular and Cellular Research Pathway.

Disclosures: Drs. Hill and Widlansky receive significant support from research grant HL128240 directly relevant to this manuscript. The authors declare they have no affiliations with or involvement in any organization or entity with any financial interest, or non-financial interest in the subject matter or materials discussed in this manuscript.

Supplemental Materials:

Expanded Results
Supplemental Tables 1-6
Supplemental Figures 1-9

References:

1. Shenouda SM, Widlansky ME, Chen K, Xu G, Holbrook M, Tabit CE, Hamburg NM, Frame AA, Caiano TL, Kluge MA, Duess MA, Levit A, Kim B, Hartman ML, Joseph L, Shirihai OS and Vita JA. Altered mitochondrial dynamics contributes to endothelial dysfunction in diabetes mellitus. *Circulation*. 2011;124:444-453.
2. Kizhakekuttu TJ, Wang J, Dharmashankar K, Ying R, Gutterman DD, Vita JA and Widlansky ME. Adverse alterations in mitochondrial function contribute to type 2 diabetes mellitus-related endothelial dysfunction in humans. *Arterioscler Thromb Vasc Biol*. 2012;32:2531-2539.
3. El-Osta A, Brasacchio D, Yao D, Pocai A, Jones PL, Roeder RG, Cooper ME and Brownlee M. Transient high glucose causes persistent epigenetic changes and altered gene expression during subsequent normoglycemia. *J Exp Med*. 2008;205:2409-2417.
4. Wang J, Alexanian A, Ying R, Kizhakekuttu TJ, Dharmashankar K, Vasquez-Vivar J, Gutterman DD and Widlansky ME. Acute Exposure to Low Glucose Rapidly Induces Endothelial Dysfunction and Mitochondrial Oxidative Stress: Role for AMP Kinase. *Arterioscler Thromb Vasc Biol*. 2012;32:712-720.
5. Yusuf S, Dagenais G, Pogue J, Bosch J and Sleight P. Vitamin E supplementation and cardiovascular events in high-risk patients. The Heart Outcomes Prevention Evaluation Study Investigators. *N Engl J Med*. 2000;342:154-160.
6. Willcox BJ, Curb JD and Rodriguez BL. Antioxidants in cardiovascular health and disease: key lessons from epidemiologic studies. *Am J Cardiol*. 2008;101:75D-86D.
7. Widlansky ME and Hill RB. Mitochondrial regulation of diabetic vascular disease: an emerging opportunity. *Transl Res*. 2018.
8. Tanner MJ, Wang J, Ying R, Suboc TB, Malik M, Couillard A, Branum A, Puppala V and Widlansky ME. Dynamin-related protein 1 mediates low glucose-induced endothelial dysfunction in human arterioles. *Am J Physiol Heart Circ Physiol*. 2017;312:H515-H527.
9. Kim H, Scimia MC, Wilkinson D, Trelles RD, Wood MR, Bowtell D, Dillin A, Mercola M and Ronai ZA. Fine-tuning of Drp1/Fis1 availability by AKAP121/Siah2 regulates mitochondrial adaptation to hypoxia. *Mol Cell*. 2011;44:532-544.
10. Kumari S, Anderson L, Farmer S, Mehta SL and Li PA. Hyperglycemia alters mitochondrial fission and fusion proteins in mice subjected to cerebral ischemia and reperfusion. *Transl Stroke Res*. 2012;3:296-304.
11. Ciarlo L, Manganelli V, Garofalo T, Matarrese P, Tinari A, Misasi R, Malorni W and Sorice M. Association of fission proteins with mitochondrial raft-like domains. *Cell Death Differ*. 2010;17:1047-1058.
12. Kaddour-Djebbar I, Choudhary V, Brooks C, Ghazaly T, Lakshmikanthan V, Dong Z and Kumar MV. Specific mitochondrial calcium overload induces mitochondrial fission in prostate cancer cells. *Int J Oncol*. 2010;36:1437-1444.
13. Widlansky ME, Jensen DM, Wang J, Liu Y, Geurts AM, Kriegel AJ, Liu P, Ying R, Zhang G, Casati M, Chu C, Malik M, Branum A, Tanner MJ, Tyagi S, Usa K and Liang M. miR-29 contributes to normal endothelial function and can restore it in cardiometabolic disorders. *EMBO Mol Med*. 2018.
14. American Diabetes A. 2. Classification and Diagnosis of Diabetes: Standards of Medical Care in Diabetes-2019. *Diabetes Care*. 2019;42:S13-S28.
15. Suboc TM, Dharmashankar K, Wang J, Ying R, Couillard A, Tanner MJ and Widlansky ME. Moderate Obesity and Endothelial Dysfunction in Humans: Influence of Gender and Systemic Inflammation. *Physiol Rep*. 2013;1.

16. Mohandas A, Suboc TB, Wang J, Ying R, Tarima S, Dharmashankar K, Malik M and Widlansky ME. Mineralocorticoid exposure and receptor activity modulate microvascular endothelial function in African Americans with and without hypertension. *Vasc Med*. 2015.
17. Egner JM, Jensen DR, Olp MD, Kennedy NW, Volkman BF, Peterson FC, Smith BC and Hill RB. Development and Validation of 2D Difference Intensity Analysis for Chemical Library Screening by Protein-Detected NMR Spectroscopy. *Chembiochem*. 2018;19:448-458.
18. Delaglio F, Grzesiek S, Vuister GW, Zhu G, Pfeifer J and Bax A. NMRPipe: a multidimensional spectral processing system based on UNIX pipes. *J Biomol NMR*. 1995;6:277-93.
19. Masse JE and Keller R. AutoLink: automated sequential resonance assignment of biopolymers from NMR data by relative-hypothesis-prioritization-based simulated logic. *J Magn Reson*. 2005;174:133-51.
20. Xu J and Van Doren SR. Binding Isotherms and Time Courses Readily from Magnetic Resonance. *Anal Chem*. 2016;88:8172-8.
21. Xu J, Sarma AVS, Wei Y, Beamer LJ and Van Doren SR. Multiple Ligand-Bound States of a Phosphohexomutase Revealed by Principal Component Analysis of NMR Peak Shifts. *Sci Rep*. 2017;7:5343.
22. Royer CA, Mann CJ and Matthews CR. Resolution of the fluorescence equilibrium unfolding profile of trp aporepressor using single tryptophan mutants. *Protein Sci*. 1993;2:1844-52.
23. Serasinghe MN, Seneviratne AM, Smrcka AV and Yoon Y. Identification and characterization of unique proline-rich peptides binding to the mitochondrial fission protein hFis1. *J Biol Chem*. 2010;285:620-30.
24. Chen H and Chan DC. Mitochondrial dynamics--fusion, fission, movement, and mitophagy--in neurodegenerative diseases. *Hum Mol Genet*. 2009;18:R169-R176.
25. Chan DC. Fusion and fission: interlinked processes critical for mitochondrial health. *Annu Rev Genet*. 2012;46:265-287.
26. Detmer SA and Chan DC. Functions and dysfunctions of mitochondrial dynamics. *Nat Rev Mol Cell Biol*. 2007;8:870-9.
27. Suen DF, Norris KL and Youle RJ. Mitochondrial dynamics and apoptosis. *Genes Dev*. 2008;22:1577-90.
28. Yu T, Robotham JL and Yoon Y. Increased production of reactive oxygen species in hyperglycemic conditions requires dynamic change of mitochondrial morphology. *Proc Natl Acad Sci U S A*. 2006;103:2653-2658.
29. Molina AJ, Wikstrom JD, Stiles L, Las G, Mohamed H, Elorza A, Walzer G, Twig G, Katz S, Corkey BE and Shirihai OS. Mitochondrial networking protects beta-cells from nutrient-induced apoptosis. *Diabetes*. 2009;58:2303-15.
30. Jheng HF, Tsai PJ, Guo SM, Kuo LH, Chang CS, Su IJ, Chang CR and Tsai YS. Mitochondrial fission contributes to mitochondrial dysfunction and insulin resistance in skeletal muscle. *Mol Cell Biol*. 2012;32:309-19.
31. Nishikawa T, Edelstein D, Du XL, Yamagishi S, Matsumura T, Kaneda Y, Yorek MA, Beebe D, Oates PJ, Hammes HP, Giardino I and Brownlee M. Normalizing mitochondrial superoxide production blocks three pathways of hyperglycaemic damage. *Nature*. 2000;404:787-790.
32. Liu N, Wu J, Zhang L, Gao Z, Sun Y, Yu M, Zhao Y, Dong S, Lu F and Zhang W. Hydrogen Sulphide modulating mitochondrial morphology to promote mitophagy in endothelial cells under high-glucose and high-palmitate. *J Cell Mol Med*. 2017;21:3190-3203.
33. Gioscia-Ryan RA, Battson ML, Cuevas LM, Zigler MC, Sindler AL and Seals DR. Voluntary aerobic exercise increases arterial resilience and mitochondrial health with aging in mice. *Aging (Albany NY)*. 2016;8:2897-2914.

34. Choi HY, Park JH, Jang WB, Ji ST, Jung SY, Kim da Y, Kang S, Kim YJ, Yun J, Kim JH, Baek SH and Kwon SM. High Glucose Causes Human Cardiac Progenitor Cell Dysfunction by Promoting Mitochondrial Fission: Role of a GLUT1 Blocker. *Biomol Ther (Seoul)*. 2016;24:363-70.
35. Zhang Y, Feng J, Wang Q, Zhao S, Yang S, Tian L, Meng P, Li J and Li H. Hyperglycaemia Stress-Induced Renal Injury is Caused by Extensive Mitochondrial Fragmentation, Attenuated MKP1 Signalling, and Activated JNK-CaMKII-Fis1 Biological Axis. *Cell Physiol Biochem*. 2018;51:1778-1798.
36. Loson OC, Song Z, Chen H and Chan DC. Fis1, Mff, MiD49, and MiD51 mediate Drp1 recruitment in mitochondrial fission. *Mol Biol Cell*. 2013;24:659-67.
37. Zinman B, Wanner C, Lachin JM, Fitchett D, Bluhmki E, Hantel S, Mattheus M, Devins T, Johansen OE, Woerle HJ, Broedl UC, Inzucchi SE and Investigators E-RO. Empagliflozin, Cardiovascular Outcomes, and Mortality in Type 2 Diabetes. *N Engl J Med*. 2015;373:2117-28.
38. Wanner C, Inzucchi SE, Lachin JM, Fitchett D, von Eynatten M, Mattheus M, Johansen OE, Woerle HJ, Broedl UC, Zinman B and Investigators E-RO. Empagliflozin and Progression of Kidney Disease in Type 2 Diabetes. *N Engl J Med*. 2016;375:323-34.
39. Mizuno M, Kuno A, Yano T, Miki T, Oshima H, Sato T, Nakata K, Kimura Y, Tanno M and Miura T. Empagliflozin normalizes the size and number of mitochondria and prevents reduction in mitochondrial size after myocardial infarction in diabetic hearts. *Physiol Rep*. 2018;6:e13741.
40. Wang Q, Zhang M, Torres G, Wu S, Ouyang C, Xie Z and Zou MH. Metformin Suppresses Diabetes-Accelerated Atherosclerosis via the Inhibition of Drp1-Mediated Mitochondrial Fission. *Diabetes*. 2017;66:193-205.
41. Liu H, Xiang H, Zhao S, Sang H, Lv F, Chen R, Shu Z, Chen AF, Chen S and Lu H. Vildagliptin improves high glucose-induced endothelial mitochondrial dysfunction via inhibiting mitochondrial fission. *J Cell Mol Med*. 2019;23:798-810.
42. Yu R, Jin SB, Lendahl U, Nister M and Zhao J. Human Fis1 regulates mitochondrial dynamics through inhibition of the fusion machinery. *EMBO J*. 2019;38.
43. Bach D, Pich S, Soriano FX, Vega N, Baumgartner B, Oriola J, Daugaard JR, Lloberas J, Camps M, Zierath JR, Rabasa-Lhoret R, Wallberg-Henriksson H, Laville M, Palacin M, Vidal H, Rivera F, Brand M and Zorzano A. Mitofusin-2 determines mitochondrial network architecture and mitochondrial metabolism. A novel regulatory mechanism altered in obesity. *J Biol Chem*. 2003;278:17190-7.
44. Lugus JJ, Ngoh GA, Bachschmid MM and Walsh K. Mitofusins are required for angiogenic function and modulate different signaling pathways in cultured endothelial cells. *J Mol Cell Cardiol*. 2011;51:885-893.

Figure Legends:

Figure 1: Vasodilation improved with Fis1 transfection compared to control (siRNA) with increased response to acetylcholine under both high and low glucose conditions. **A.** Impact of molecular inhibition of Fis1 expression on endothelial vasodilation under high glucose conditions. The impaired vasodilation caused by high glucose conditions was improved under Fis1 knockdown conditions (P=0.0002 overall, *P≤0.0002 at indicated Ach doses for control siRNA vs Fis1 siRNA, N=6 subjects). L-NAME could abolish this improvement of vasodilation under Fis1 knockdown conditions (P<0.0001 for Fis1 siRNA vs siFis1+L-NAME and P=0.002 for control siRNA vs control siRNA+L-NAME). **B.** Impact of molecular knockdown of Fis1 expression on endothelial vasodilation under low glucose conditions. The impaired vasodilation caused by low glucose conditions was improved under Fis1 knockdown conditions (P=0.0008 overall, *P≤0.0003 at indicated Ach doses for control siRNA vs Fis1 siRNA, N=6 subjects). L-NAME could abolish this improvement of vasodilation under Fis1 knockdown conditions (P=0.0002 for Fis1 siRNA vs Fis1 siRNA+L-NAME). Ach- Acetylcholine.

Figure 2: The bioavailability of NO increased in human arterioles with reduction of Fis1 levels under high and low glucose conditions. A. Low glucose (LG): (n=8, overall P=0.01; P=0.03 for control siRNA vs. Fis1 siRNA; P=0.003 for control siRNA+L-NAME vs Fis1 siRNA; P=0.03 for Fis1 siRNA vs Fis1 siRNA+L-NAME. Box represents 25 and 75 percentiles. Horizontal line represents the median. **B.** High Glucose: (n=9, overall P=0.04; P=0.01 for scrambled siRNA vs Fis1 siRNA; P=0.03 for Fis1 siRNA vs control siRNA+L-NAME and P=0.047 for Fis1 siRNA vs Fis1 siRNA+L-NAME).

Figure 3: Suppression of Fis1 expression in DM arterioles reversed impaired endothelium-dependent vasodilation (n=6, P=0.002 overall). L-NAME blocked this effect

(P<0.0004 for Fis1 siRNA vs Fis1 siRNA+L-NAME). * P<0.0005 for vs. all other exposures at the indicated Ach doses. Ach-acetylcholine

Figure 4: Molecular inhibition of Fis1 under high glucose (33mM) and low glucose (2.5mM) conditions improved steady-state junction stability between endothelial cells in the monolayer. Comparison of electric cell-substrate impedance sensing measurements (ECIS) in human microvascular endothelial cells (HMEC-1) transfected with Fis1 siRNA and control siRNA between high and normal Glucose conditions **(A)** and normal and low glucose conditions **(B)**. Box represents 25th to 75th percentiles. Horizontal line represents the median. SANOVA followed by Tukey's multiple comparison test, n=4 for each treatment (P<0.001 overall for both high and low glucose studies. *-P<0.05, **P<0.01, ***P<0.001, ****P<0.0001. HG- High glucose, LG- Low Glucose, NG- Normal Glucose

Figure 5: **Molecular inhibition of Fis1 under high glucose (33mM) and low glucose (2.5mM) conditions did not alter mitochondrial bioenergetics compared to normal Glucose (5mM) conditions.** Measures of extracellular acidification rate (ECAR, n=5) **(A)** and oxygen consumption rate (OCR, n=5) **(B)** in human microvascular endothelial cells (HMEC-1) transfected with Fis1 siRNA and control siRNA pre-incubated with high glucose (6 hours), normal glucose (5mM for 2 hours), and low glucose (2 hours). Wild type (WT) cells represent HMEC-1 cells not transfected and grown under normal glucose conditions. ECAR and OCR were measured under basal conditions followed by the sequential addition of oligomycin (2.5 µM), FCCP (1 µM), as well as rotenone (1 µM) and antimycin A (1 µM). No statistically significant differences were present between the treatments.

Figure 6: Novel peptide pep213 binding to Fis1. (A)1H, 15N HSQC spectral overlay of a 50 µM 15N-Fis1 sample titrated with increasing amounts (0-2000µM) of unlabeled p213 demonstrating significant chemical shift indicating affinity of p213 for Fis 1. (B) Affinity

determination for pep213 binding to Fis1 from NMR data in (A) by applying TREND analysis to all spectra in the titration series and fitting the normalized principal component 1 values (PC1) to a ligand depletion model to determine an apparent KD = 7 ± 2 µM. (C) Affinity determination by intrinsic tryptophan fluorescence. Fis1 containing a single tryptophan was titrated with increasing amounts (0-1000 µM) of pep213 that contains no tryptophan. The average emission wavelength was determined and fit to determine an apparent KD = 3.3 ± 0.1 µM. Residuals to the fits in panels B and C are shown in the top of each panel. (D) 1H, 15N HSQC spectral overlay of a 50 µM 15N-Fis1 sample titrated with 2000µM of a scrambled peptide with the same amino acids as p213 demonstrating no significant chemical shift indicating no affinity of a scrambled peptide for Fis 1.

Figure 7: Pep213-tat reverses impaired endothelium dependent vasodilation in healthy human vessels exposed to high glucose and in vessels from humans with T2DM.

(A) High glucose induced impairment of endothelium-dependent vasodilation to acetylcholine was reversed by treatment with 1-10 µM of pep213 (n=5, P<0.0001) attached to a tat sequence to facilitate cellular entry. L-NAME reversed all improvements with pep213-tat treatment (P<0.0001 for pep 213 vs pep-213+L-NAME). *P<0.0001 at the indicated Ach concentration for pep213 vs. all other exposures). **B)** The impaired endothelium-dependent vasodilation to Ach in vessels from T2DM subjects was reversed by pep213 (P<0.001 overall, *P<0.05 at the indicated Ach concentrations for pep213 vs. all other exposures). Ach-acetycholine. T2DM- type 2 diabetes

Figure 8: pep213-tat reverses impaired endothelium dependent vasodilation in healthy human vessels exposed to high glucose and in vessels from humans with T2DM compared to scrambled peptide control. (A) Acetylcholine induced endothelium-dependent vasodilation pre-exposed to six hours of high glucose (33mM) was reversed with 1 µM pep213-

tat compared to a scrambled peptide containing the same amino acids as pep213 attached a tat sequence. (n=5, P<0.001 overall, *P<0.05 at indicated Ach concentrations). (B) Similar results were seen with vessels from T2DM subjects (n=4, P<0.001 overall, *P<0.05 at the indicated doses).

Figure 1

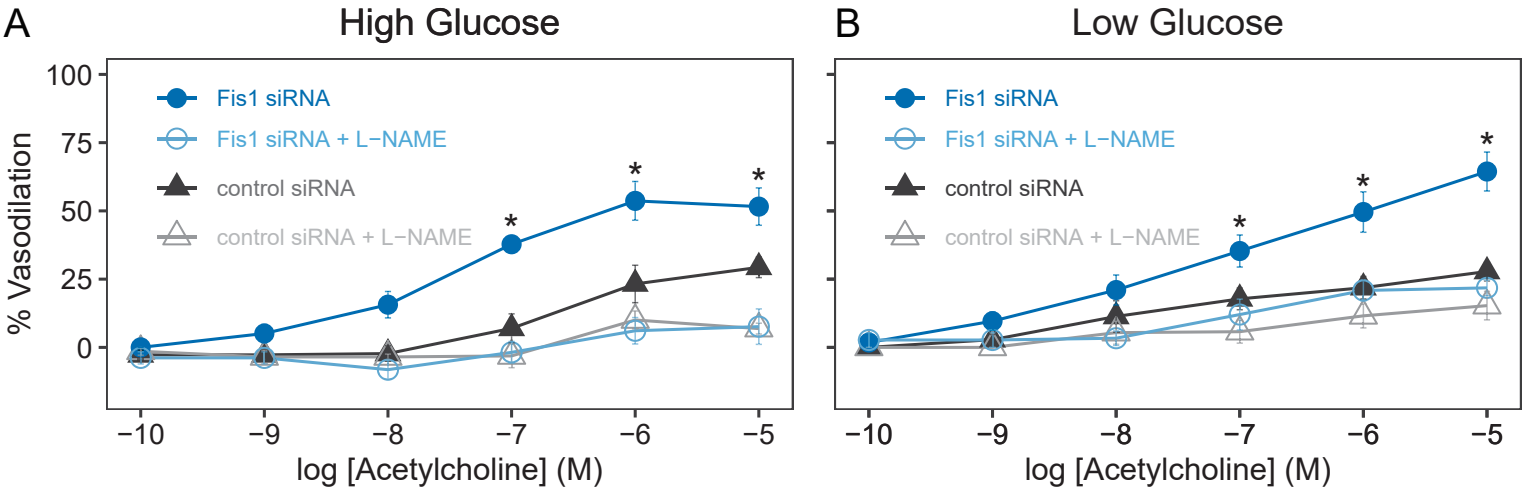
A
High Glucose
B
Low Glucose
% Vasodilation
100
75
50
25
0
Fis1 siRNA
Fis1 siRNA + L−NAME
control siRNA
control siRNA + L−NAME
*
−10
−9
−8
−7
−6
−5
log [Acetylcholine] (M)

Figure 2

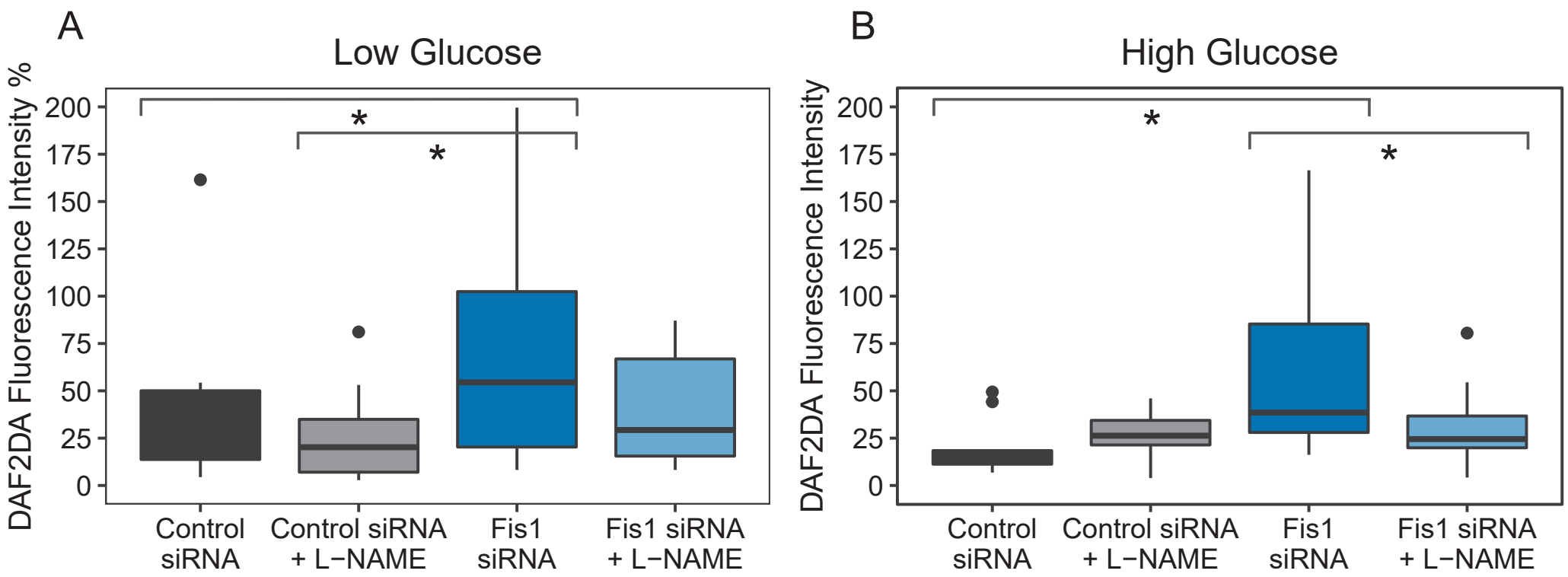
A
Low Glucose
DAF2DA Fluorescence Intensity %
200
175
150
125
100
75
50
25
0
*
*
Control siRNA
Control siRNA + L−NAME
Fis1 siRNA
Fis1 siRNA + L−NAME
B
High Glucose
DAF2DA Fluorescence Intensity
200
175
150
125
100
75
50
25
0
*
*
Control siRNA
Control siRNA + L−NAME
Fis1 siRNA
Fis1 siRNA + L−NAME

Figure 3

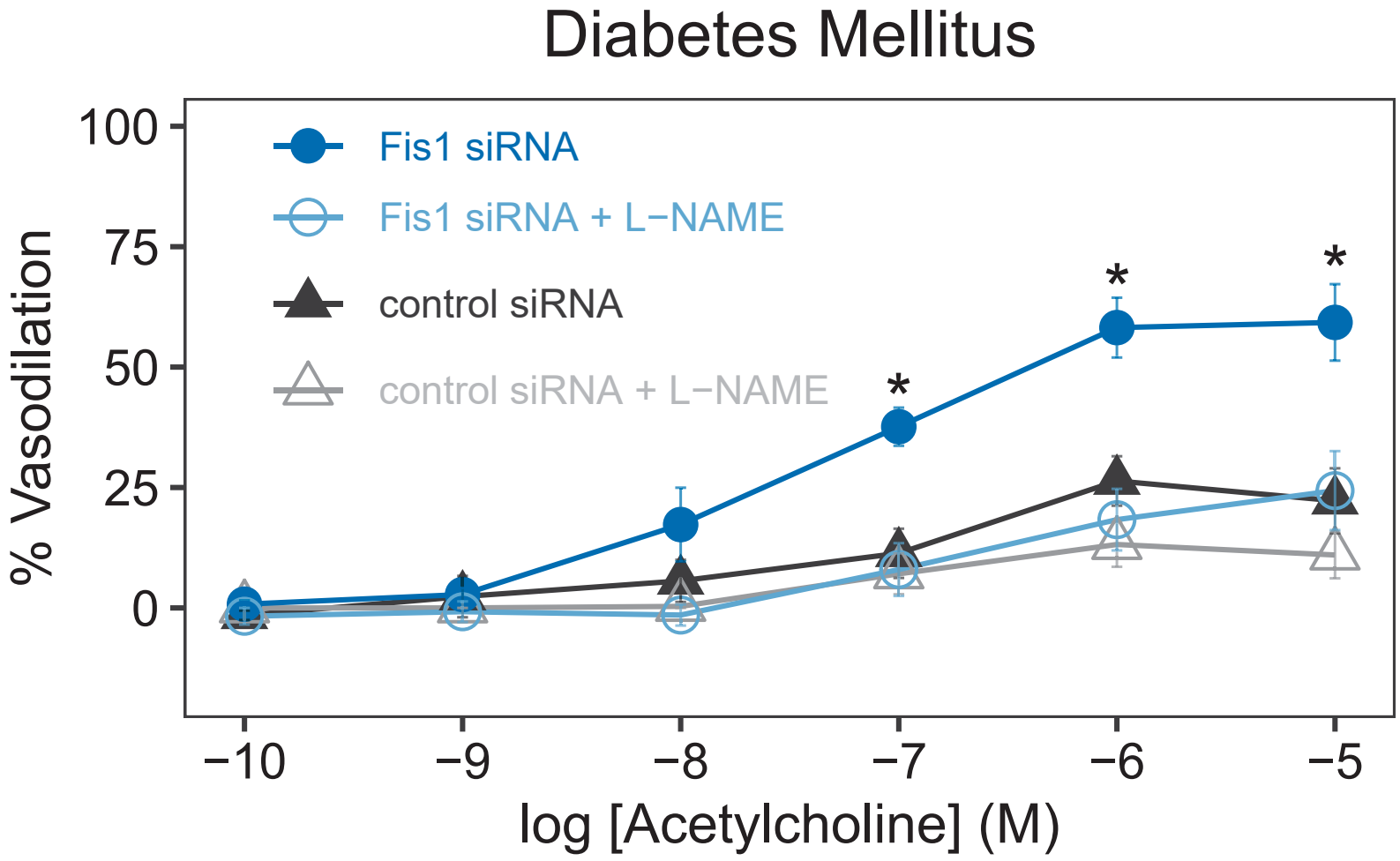
Diabetes Mellitus
Fis1 siRNA
Fis1 siRNA + L−NAME
control siRNA
control siRNA + L−NAME
% Vasodilation
100
75
50
25
0
*
*
*
−10
−9
−8
−7
−6
−5
log [Acetylcholine] (M)

Figure 4

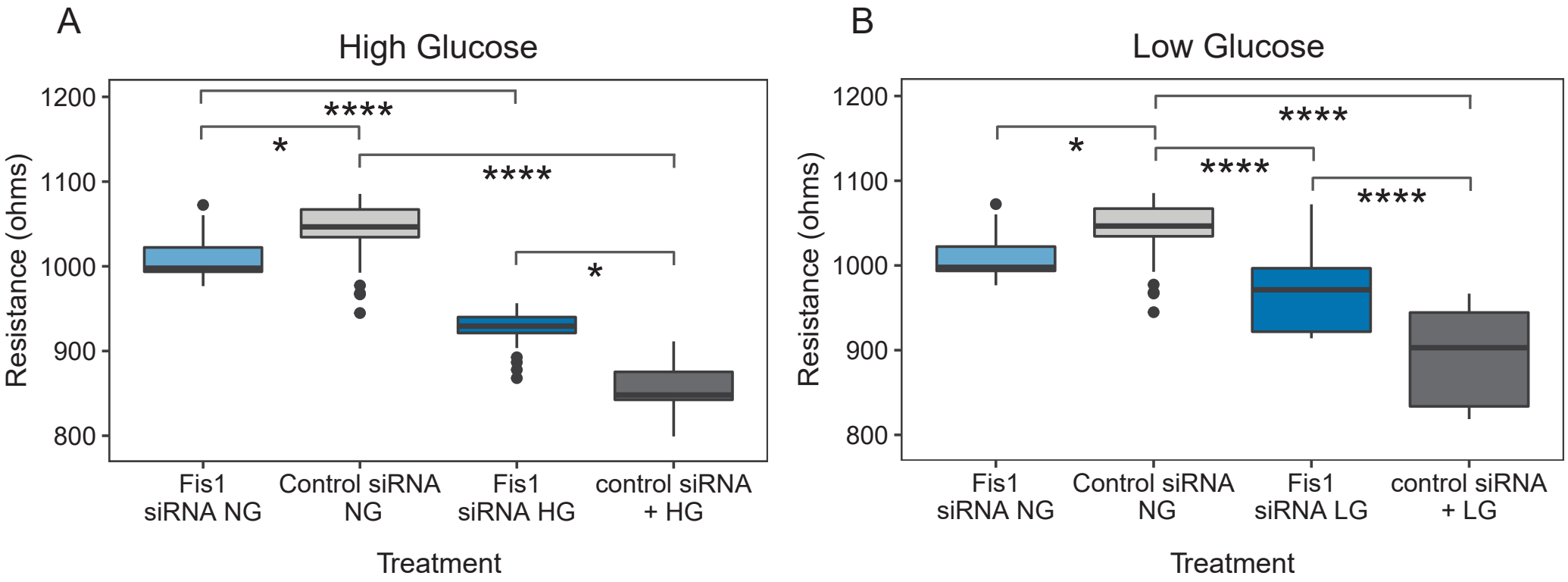
A
High Glucose
Resistance (ohms)
1200
1100
1000
900
800
****
*
****
*
Fis1 siRNA NG
Control siRNA NG
Fis1 siRNA HG
control siRNA + HG
Treatment
B
Low Glucose
Resistance (ohms)
1200
1100
1000
900
800
****
*
****
****
Fis1 siRNA NG
Control siRNA NG
Fis1 siRNA LG
control siRNA + LG
Treatment

Figure 5

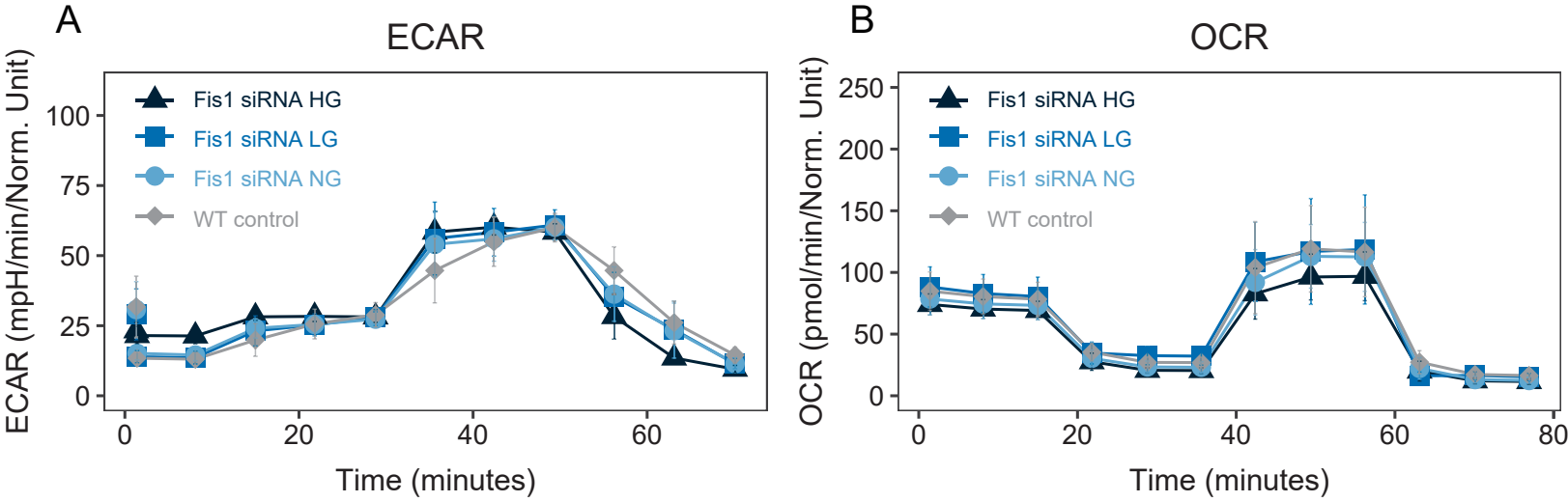
A
ECAR
ECAR (mpH/min/Norm. Unit)
Fis1 siRNA HG
Fis1 siRNA LG
Fis1 siRNA NG
WT control
0
25
50
75
100
0
20
40
60
Time (minutes)
B
OCR
OCR (pmol/min/Norm. Unit)
Fis1 siRNA HG
Fis1 siRNA LG
Fis1 siRNA NG
WT control
0
50
100
150
200
250
0
20
40
60
80
Time (minutes)

Figure 6

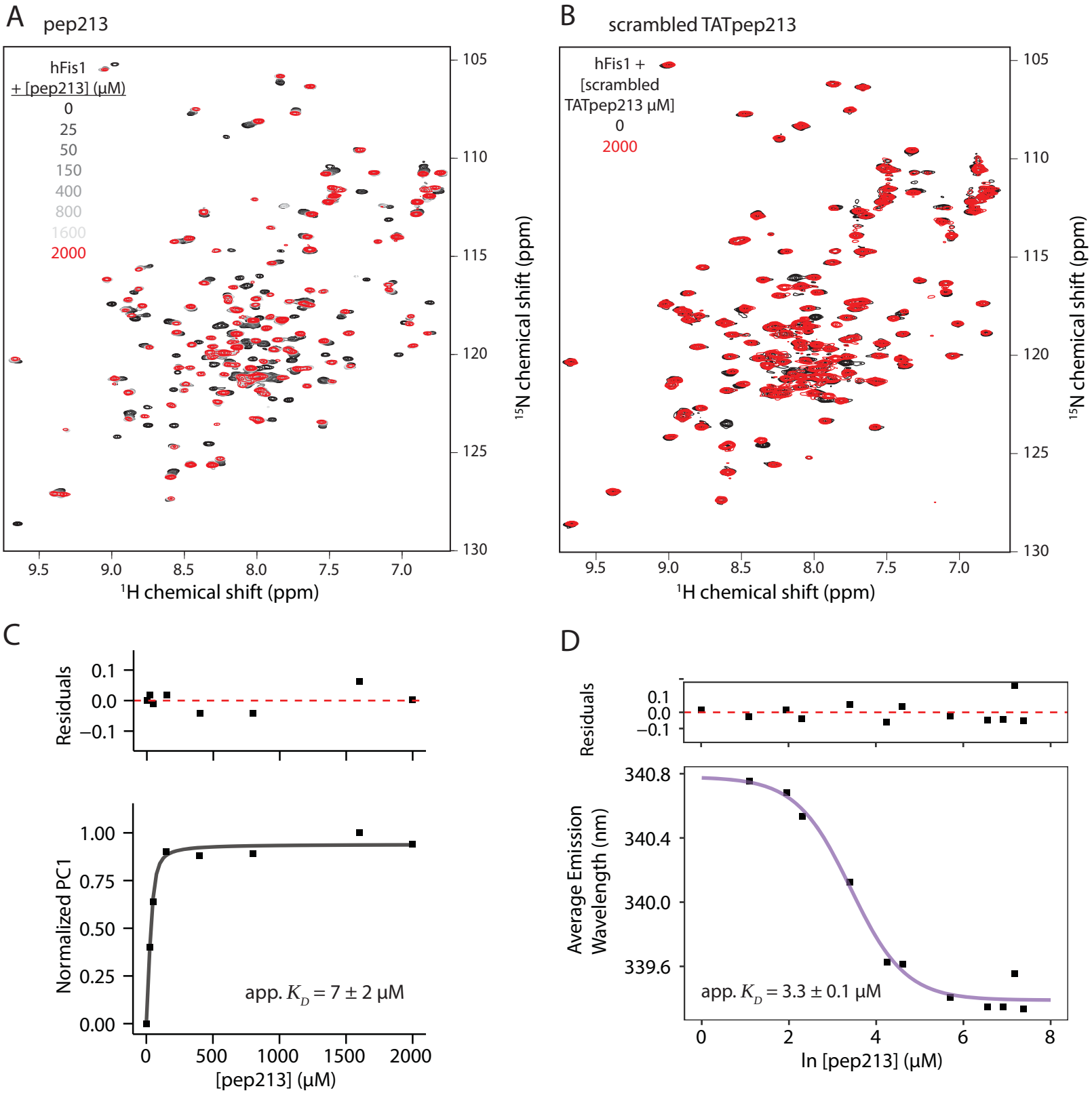
A
pep213
hFis1
+ [pep213] (μM)
0
25
50
150
400
800
1600
2000
105
110
115
120
125
130
9.5
9.0
8.5
8.0
7.5
7.0
¹H chemical shift (ppm)
¹⁵N chemical shift (ppm)
B
scrambled TATpep213
hFis1 +
[scrambled
TATpep213 μM]
0
2000
C
Residuals
0.1
0.0
−0.1
Normalized PC1
1.00
0.75
0.50
0.25
0.00
app. $K_D = 7 \pm 2$ μM
0
500
1000
1500
2000
[pep213] (μM)
D
Average Emission
Wavelength (nm)
340.8
340.4
340.0
339.6
app. $K_D = 3.3 \pm 0.1$ μM
0
2
4
6
8
ln [pep213] (μM)

Figure 7

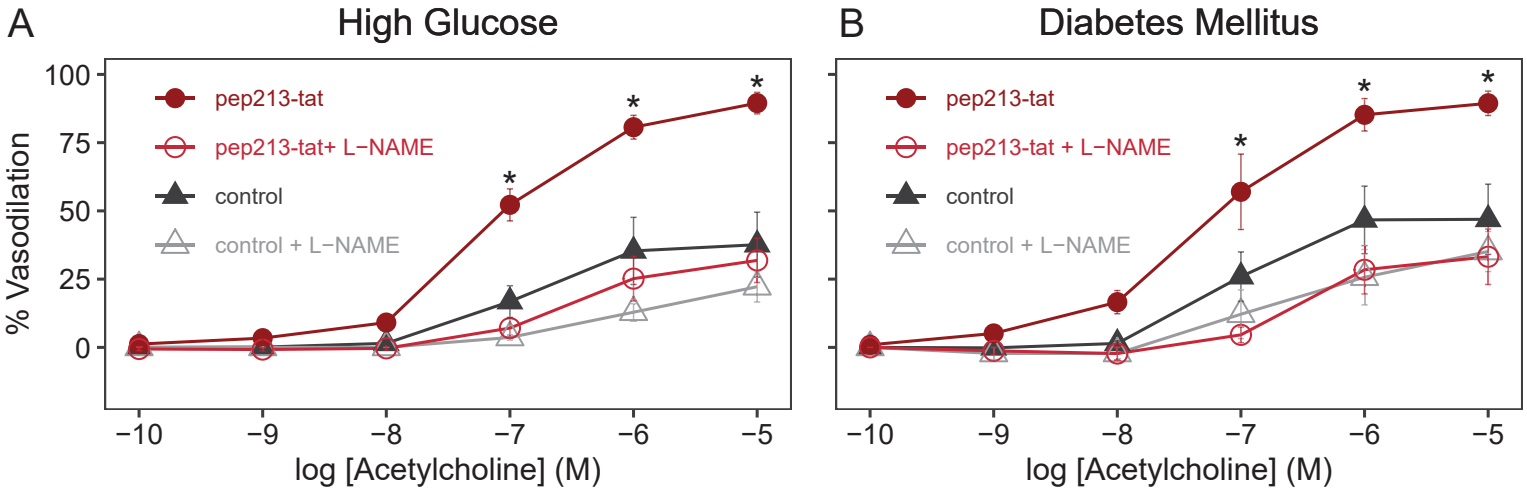
A
High Glucose
B
Diabetes Mellitus
% Vasodilation
100
75
50
25
0
pep213-tat
pep213-tat+ L−NAME
control
control + L−NAME
pep213-tat + L−NAME
*
−10
−9
−8
−7
−6
−5
log [Acetylcholine] (M)

Figure 8

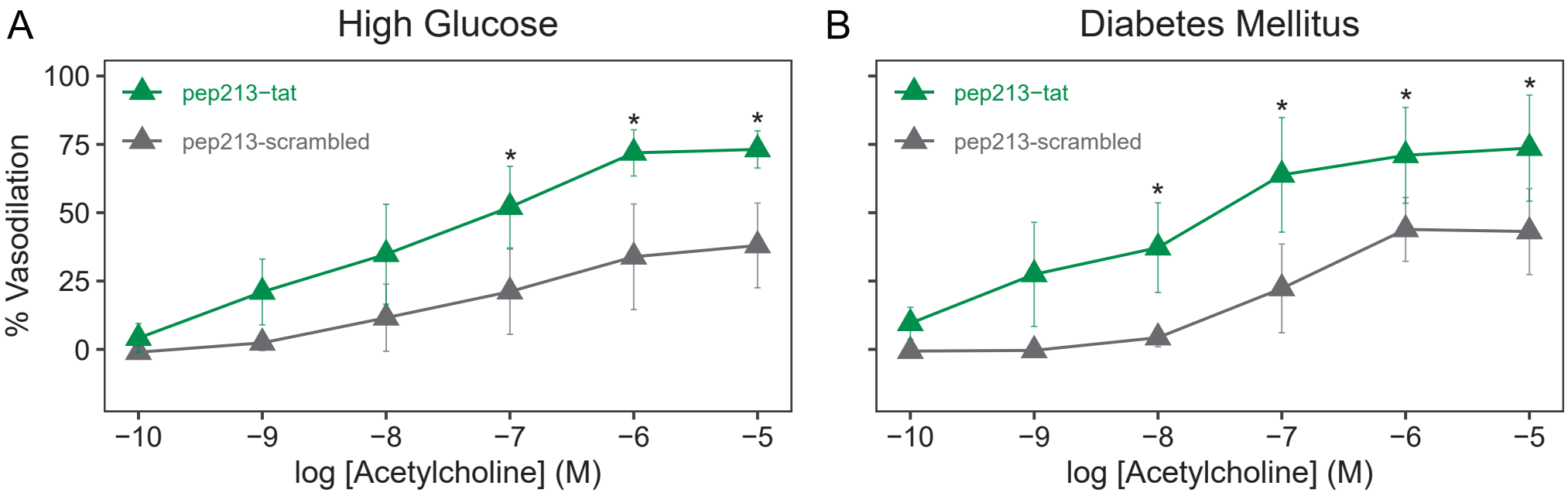
A
High Glucose
B
Diabetes Mellitus
pep213−tat
pep213-scrambled
% Vasodilation
100
75
50
25
0
−10
−9
−8
−7
−6
−5
log [Acetylcholine] (M)
*